



## Directly drawing high-performance capacitive sensors on copying tissues†

Cite this: *Nanoscale*, 2018, **10**, 17002

Received 16th July 2018,  
Accepted 20th August 2018

DOI: 10.1039/c8nr05731a

rsc.li/nanoscale

Yu-Qing Liu,<sup>a</sup> Yong-Lai Zhang,<sup>b</sup> \*<sup>a</sup> Zhi-Zhen Jiao,<sup>a</sup> Dong-Dong Han<sup>a</sup> and Hong-Bo Sun<sup>b</sup>

**We report here a facile, green and cost-effective fabrication of high-performance capacitive pressure sensors by drawing loop- and disc-shaped graphite electrode arrays on copying tissues. Graphene oxide enhanced foam-like paper is prepared as an efficient dielectric layer. The paper-based capacitive pressure sensor enables sensitive detection of finger touch, motion and proximity.**

Flexible pressure sensors that enable detection of tiny forces are promising candidates for application in intelligent devices, such as smart textiles, electronic skins, human-machine interfaces, human health monitoring and motion tracking systems, and diagnostic devices.<sup>1–8</sup> To convert mechanical deformation to electronic signals, different types of pressure sensors, for instance, piezoresistors, capacitors, piezoelectric sensors and field-effect transistors, have been successfully developed over the past few decades.<sup>9–14</sup> Among these pressure sensors, the piezoresistive-type sensor, based on mechanical deformation induced resistance changes, has emerged as a promising one due to the distinct advantage of cost-effective fabrication, as well as ease of signal collection/readout.<sup>15–18</sup> Taking advantage of the softness and elasticity of rubber or low-modulus elastomers, flexible and stretchable piezoresistive sensors have been successfully prepared by embedding various conductive dopants (*e.g.*, carbon nanotubes, graphene, and silver nanowires).<sup>19–23</sup> However, this type of sensors usually suffer from poor sensitivity and high operating pressure, which limit their application in wearable electronic skins. To achieve a high sensitivity and a broad detecting regime, graphene-based aerogels,<sup>24</sup> foam<sup>25</sup> and honeycomb-like films<sup>26</sup> have been pre-

pared as sensing materials, revealing their great potential for developing piezoresistive-type pressure sensors.

Considering their capability of detecting proximity and their better compatibility with wireless detection systems,<sup>27–30</sup> capacitive-type sensors could be more valuable than resistive-type ones. For capacitive-type pressure sensors, the variation of capacitance can be utilized for pressure sensing. Thus, the flexibility of the electrodes and the effective relative dielectric permittivity of the capacitor that can be changed under pressure are crucial to sensitivity. Following this line, several typical flexible pressure sensors have recently been reported. For instance, Sun *et al.* presented an ultrasensitive capacitive pressure sensor using reduced graphene oxide (RGO) at polyethylene terephthalate (PET) as the electrodes and graphene oxide (GO) foam as the high-performance dielectric material.<sup>31</sup> Ahn *et al.* reported a graphene-based three-dimensional capacitive touch sensor with good sensing capabilities in both the contact and noncontact modes using graphene at ultrathin PET as the top/bottom electrodes and an acrylic polymer as the dielectric layer.<sup>32</sup> Shim *et al.* utilized the surface roughness of paper to fabricate high performance capacitive pressure sensors, which consist of a pair of polydimethylsiloxane (PDMS) coated graphite electrodes.<sup>33</sup> Madden *et al.* developed bendable, stretchable, and transparent touch sensors that enable locating a finger based on a cross-grid array of ionically conductive hydrogel electrodes embedded in a silicone elastomer.<sup>34</sup> However, despite the fact that the abovementioned capacitive-type pressure sensors have demonstrated high sensitivity, a large detection region and the capability to achieve non-contact detection of proximity, current strategies for producing such high performance sensors still involve complex fabrication procedures and the use of polymers and costly materials. At present, a green, facile and cost-effective fabrication of high-performance flexible pressure sensors is highly desired, but it remains a challenging task.

In this paper, we report the fabrication of paper-based capacitive pressure sensors by pencil drawing of loop- and disc-shaped graphite electrode arrays on copying tissue sheets. Graphene oxide (GO)-enhanced foam-like paper, prepared by

<sup>a</sup>State Key Laboratory of Integrated Optoelectronics, College of Electronic Science and Engineering, Jilin University, 2699 Qianjin Street, Changchun, 130012, China. E-mail: yonglaizhang@jlu.edu.cn

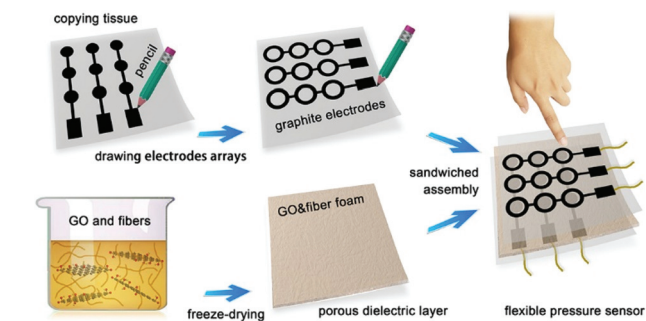
<sup>b</sup>State Key Laboratory of Precision Measurement Technology & Instruments, Department of Precision Instrument, Tsinghua University, Haidian district, Beijing 100084, China

†Electronic supplementary information (ESI) available. See DOI: 10.1039/c8nr05731a

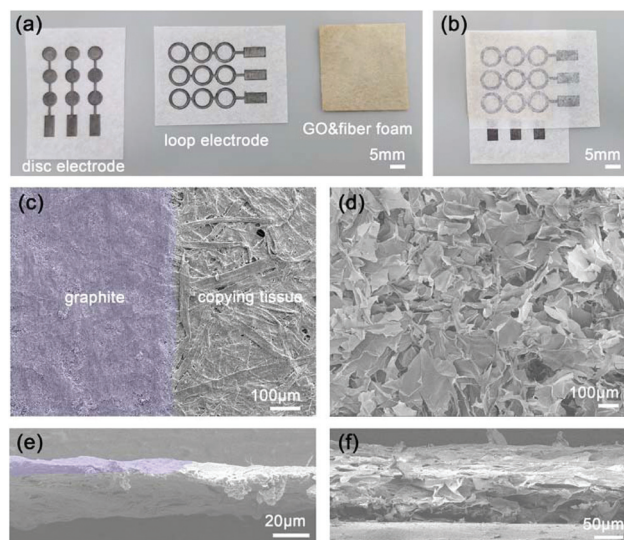
freeze-drying of paper cellulose fibers and GO composites, was employed as a high-performance dielectric layer. The whole fabrication process is simple, green and cost-effective, and the obtained capacitive pressure sensors are highly sensitive to pressure and approaching objects, enabling detection of finger motion, touching and proximity.

Fig. 1 shows a schematic illustration of the fabrication of our paper-based pressure sensor. In our work, soft, thin and robust copying tissues have been employed for sensor fabrication. Fig. S1† shows a photograph of a single sheet of copying tissue; the paper is so thin that it is semi-transparent. The thickness was found to be  $\sim 22 \mu\text{m}$ . To make the fabrication process simple, green and cost-effective, we prepared the top and bottom electrodes by pencil drawing. To obtain a sensitive electric field that can be affected by both pressure and proximity, we designed disc- and loop-shaped graphite electrode arrays as cross-grid electrodes. The dielectric layer was also prepared from paper. We first broke the Kleenex into cellulose fibers in water with the help of ultrasonic treatment. Then, the cellulose fiber solution was mixed with GO and freeze-dried to form a porous foam, which is used as the dielectric layer. The presence of GO can promote the porosity and mechanical strength of the foam. The capacitive pressure sensor was fabricated by the sandwiched assembly of top/bottom electrode layers with a GO&fiber foam layer.

Fig. 2 shows photographs and scanning electron microscopy (SEM) images of the bottom/top electrodes and the dielectric layer. We drew a  $3 \times 3$  disc-electrode array and a  $3 \times 3$  loop electrode array on two separate copying tissues, respectively. Then, a GO&fiber foam paper was cut into a square shape with a size that can cover the  $3 \times 3$  loop electrode array. The assembly of the device is also very simple. As shown in Fig. 2b, we just sandwiched the dielectric layer of GO&fiber foam paper between the two graphite electrodes on copying tissues, with the loop electrode on top. To obtain detailed morphology information, we characterized both the electrodes and the dielectric layer by SEM. The cellulose fibers of the copying tissue can be clearly identified at the surface, whereas the pencil-drawn region (marked in color) is smooth, since graph-



**Fig. 1** Schematic illustration of the fabrication of a pressure sensor with pencil drawn graphite electrodes and GO&fiber foam paper as the dielectric layer.



**Fig. 2** (a) Photographs of a disc-shaped electrode array, a loop-shaped electrode array and the GO&fiber foam; (b) photograph of the sandwiched device structure; (c) SEM image of the graphite coated copying tissue; (d) SEM image of the GO&fiber foam paper; (e) section view of the graphite coated copying tissue; (f) section view of the GO&fiber foam paper.

ite fully covered the tissue surface. The graphite electrode is quite compact, which ensures its good stability. We further characterized the graphite electrode after pressing it hundreds of times. As shown in Fig. S2,† it is stable; it is not peeling off from the paper substrate. The roughness of the copying tissue plays an important role in the robustness of these graphite electrodes. The boundary is quite clear, and can be easily identified. The Raman spectrum confirms that, in the graphite electrode, a typical G band that corresponds to the  $\text{sp}_2$  carbon can be detected (ESI, Fig. S3).

Fig. 2d shows the SEM image of the surface of GO&fiber foam. The foam-like porous structure that consists of GO sheets and cellulose fibers can be clearly observed. The Raman spectrum of the GO&fiber foam shows typical D and G bands, confirming the presence of GO (Fig. S4†). According to the XPS spectra, both the GO and the cellulose fibers, as well as the composite foam, mainly consist of C and O. A small amount of N can be detected in the cellulose fibers and the foam (Fig. S5†). Since both the GO and the cellulose fibers are isolated, the composite foam with abundant porosity can act as a high-performance dielectric layer of the capacitive pressure sensor. Section-view SEM images of these papers show their thickness. The copying tissue is  $\sim 22 \mu\text{m}$  in thickness. Considering the roughness of the copying tissue surface, the graphite layer was  $3\text{--}5 \mu\text{m}$  (Fig. 2e). The average sheet resistance of the transferred graphite electrode is  $\sim 900 \Omega \text{sq}^{-1}$ . The GO&fiber foam was  $\sim 60 \mu\text{m}$  in thickness (Fig. 2f).

The paper-based capacitive pressure sensor can work in both the contact and noncontact modes. In the former case, we detect the capacitance change upon pressure (Fig. 3a). The porous dielectric layer of GO&fiber foam is essential for achiev-

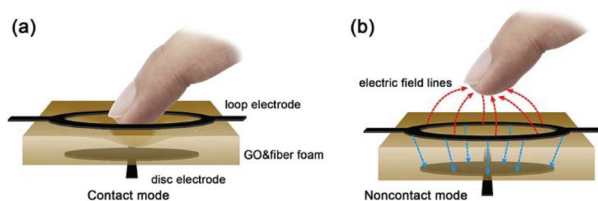


Fig. 3 Schematic illustration of (a) contact mode detection of pressure and (b) noncontact mode detection of proximity.

ing high sensitivity. First, there exist a large number of air voids within the foam. When the foam is compressed, air that has a relatively lower dielectric constant can be exhausted, leading to the increase of the dielectric constant. Meanwhile, the compression of the GO&fiber foam can also cause a decrease in the distance between the top and bottom electrodes. The synergetic effects lead to a capacitance increase, enabling sensitive detection of tiny pressure. For the noncontact detection of proximity, the disc-loop electrode structure plays a very important role. As reported by Madden *et al.*,<sup>34</sup> the disc-loop coupling enables better vertical projection of the field than simple crossing grid structures. As shown in Fig. 3b, when a finger approaches the sensor, the coupling between electrodes can be reduced due to the presence of the finger. Here the finger can be considered as a third electrode that is capacitively coupled to the sensor element. Since the mutual capacitance change is very sensitive to the location of the finger, the sensor also enables detection of finger proximity.

The pressure sensing capabilities of our paper-based capacitive pressure sensor were firstly measured in the contact mode. The operating frequency for all of the tests was fixed at 1 kHz. The pressure response curve of sensitivity is demonstrated in Fig. 4a. Here, the sensitivity (denoted as  $S$ ) is calculated according to the equation:

$$S = d(\Delta C/C_0)/dp$$

where  $C$  and  $C_0$  are the corresponding capacitances with and without pressure, and  $p$  is the applied pressure. Notably, the paper-based capacitive pressure sensor shows a high sensitivity of  $\sim 0.63 \text{ kPa}^{-1}$  at the low pressure regime (0–2 kPa), revealing the capability of detecting tiny pressure. With the increase of the applied pressure, the sensitivity decreased slightly to  $\sim 0.14 \text{ kPa}^{-1}$ . The difference in sensitivity can be attributed to the gradually increased elastic resistance, which depends on the density of the foams, *i.e.* different air/foam volume ratios. At the low pressure regime, the density of the foams is very low, so that a subtle pressure can induce an obvious change in the capacitance, corresponding to a high sensitivity. When the density of the foam becomes higher and higher, the same change in the capacitance needs much larger pressure, which results in a decrease in sensitivity. To demonstrate the unique merits of the copying tissue, we also fabricated other similar sensors using printing paper and newspaper. The resultant sensors show much lower sensitivity (Fig. S6†). In addition, our paper-based capacitive pressure sensor also features a fast

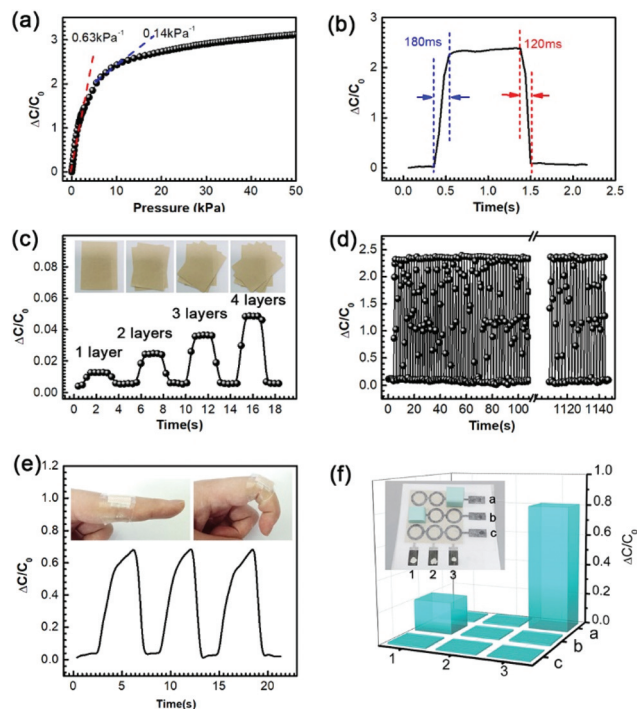


Fig. 4 (a) Capacitive response as a function of pressure; (b) response and relaxation times during the loading and unloading process; (c) stability of the capacitive response during the loading and unloading process over 70 cycles; (d) capacitive response to tiny pressures measured by loading kraft papers of different layers; (e) capacitive response of the sensor during the bending and unbending of a finger for three cycles. The inset shows photographs of a finger wearing a paper-based pressure sensor at the knuckle; (f) pressure map with column height corresponding to the relative capacitance changes. The inset shows a photograph of the  $3 \times 3$  pressure sensor array loaded with two rubber blocks corresponding to pressure values of 0.3 and 1.0 kPa, respectively.

response and relaxation time. As shown in Fig. 4b, the response and relaxation times were found to be  $\sim 180$  and  $120$  ms, respectively. To evaluate the detection limit to tiny pressure, we applied different layers of kraft paper sheets on the sensor. Here, one layer of kraft paper corresponds to a pressure value of 1.6 Pa. In our experiment, the response to tiny pressure is almost linear at the low pressure regime. The sensor can detect 1 layer of kraft paper; thus the detection limit was evaluated to be  $\sim 1.6$  Pa. The high sensitivity of our sensor can be attributed to two factors. First, the dielectric layer of the GO&fiber foam features low elastic resistance and variable dielectric constant upon compression. Second, we used ultra-soft copying tissue as the electrode substrate instead of polymers. In addition to good sensitivity, the sensor also demonstrates good stability. After 500 loading-unloading cycles with 10 kPa, the sensor maintains its function with minimal output signal degradation (Fig. 4d). Air humidity change would affect the sensing performance. With the increase of environmental humidity, the adsorption of water by the GO&fiber dielectric layer would slightly increase the capacity. Nevertheless, it generally needs a long time to reach a

balanced capacity. In this case, the effect of humidity is not obvious. To further reduce the effect of humidity, the edges of the sensor can be sealed with tape.

Taking advantage of the thin and soft nature of copying tissue, the paper-based capacitive pressure sensor is very flexible and can be well suited for wearable devices. We integrated the sensor with a Band-aid and put it over the knuckle of a finger. In this way, the sensor enables sensitive detection of the bending and unbending motion of the finger (Fig. 4e). Besides, as a proof-of-concept, a  $3 \times 3$  multiple-pixel sensor array has been fabricated for detecting the pressure map. As shown in Fig. 4f, each of the loops is 1 cm in diameter, and the spacing between pixels is 2 mm. We applied two rubber blocks (corresponding to pressure values of 0.3 and 1.0 kPa) to the surface of the sensor array (positions b-1 and a-3), and the capacitive responses of 0.2 and 0.8 in  $\Delta C/C_0$  have been detected.

In addition to contact mode pressure detection, the paper-based capacitive sensor also permits detection of finger proximity. To investigate the proximity detection capability, we changed the distance ( $d$ , inset of Fig. 5a) between a hovering finger and the top of the sensor and recorded the capacitance changes. Fig. 5a shows the mutual capacitance change upon finger proximity. Typically, when a finger approaches the sensor, part of the fringing electric field can be absorbed, leading to the negative change in capacitance. With the decrease of  $d$ , the ratio between mutual capacitance and the unperturbed value decreased obviously. The sensor was demonstrated to be highly sensitive to finger proximity. When the distance is 6 cm, only  $\sim 5\%$  of capacitance change can be detected. However, when the finger approaches the sensor surface closely (almost touching the sensor), the capacitance decreases to 86.5% ( $C/C_0$ ). Further touch of the sensor by applying a tiny pressure would lead to the increase of the capacitance; in this case, the sensor may work in the contact mode. When two fingers approached the  $3 \times 3$  multiple-pixel sensor array (with one finger pressing one pixel and the other finger hovering at a small distance), we recorded the capacitance of each pixel. Fig. 5b shows the map of the capacitance

change of each sensing pixel. Under finger press (a-3), a capacitance increase of 1.3 in  $\Delta C/C_0$ , corresponding to 2.1 kPa of pressure, can be detected. With a hovering finger, the sensing pixel of a-1 demonstrates a capacitance response of 0.11 in  $\Delta C/C_0$ .

## Conclusions

In conclusion, paper-based capacitive pressure sensors have been successfully developed using a facile, green and cost-effective pencil drawing method. The use of copying tissue is essential for achieving high sensing performance, since this kind of paper is thin, soft and robust. Besides, to develop a high-performance dielectric layer, a foam-like porous paper has been prepared by freeze-drying of paper cellulose fibers and GO composites. By designing a disc- and loop-electrode array, the capacitive sensor enables detection of both finger touch and proximity. Under the contact sensing mode, the pressure sensor shows a high sensitivity of  $0.63 \text{ kPa}^{-1}$  and fast response/relaxation time, as well as a satisfactory detection limit. Under the noncontact sensing mode, the capacitive sensor permits sensitive detection of finger proximity. It is believable that the high performance capacitive sensors fabricated through such a simple method may find broad applications in various intelligent devices, such as wearable electronics, human-machine interfaces, and health monitoring systems.

## Conflicts of interest

There are no conflicts to declare.

## Acknowledgements

The authors acknowledge the National Key Research and Development Program of China and the National Natural Science Foundation of China for support under Grant No. 2017YFB1104300, 61522503, 61590930, 61775078, and 61605055.

## References

- 1 Z. Wang, L. Zhang, J. Liu, H. Jiang and C. Li, *Nanoscale*, 2018, **10**, 10691–10698.
- 2 D. D. Han, Y. L. Zhang, J. N. Ma, Y. Q. Liu, B. Han and H. B. Sun, *Adv. Mater.*, 2016, **28**, 8328–8343.
- 3 J. N. Wang, Y. Q. Liu, Y. L. Zhang, J. Feng, H. Wang, Y. H. Yu and H. B. Sun, *Adv. Funct. Mater.*, 2018, **28**, 1800625.
- 4 D. L. Gao, W. Q. Ding, M. Nieto-Vesperinas, X. M. Ding, M. Rahman, T. H. Zhang, C. Lim and C. W. Qiu, *Light: Sci. Appl.*, 2017, **6**, e17039.
- 5 S. Seo, C. Allain, J. Na, S. Kim, X. Yang, C. Park, J. Malinge, P. Audebert and E. Kim, *Nanoscale*, 2013, **5**, 7321–7327.

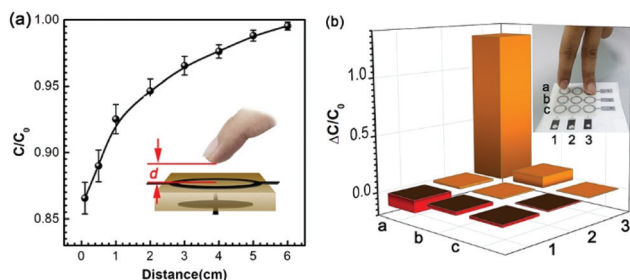


**Fig. 5** Capacitive response of the paper-based sensor for finger proximity and touching. (a) Capacitive change ( $C/C_0$ ) versus distance,  $d$ , between the sensor and the finger. The inset shows the scheme for  $d$ ; (b) a  $3 \times 3$  multiple-pixel sensor array for detecting both finger proximity and touching. The column height corresponds to the relative capacitance changes. The inset shows a photograph of the real  $3 \times 3$  pressure sensor array under finger touching and proximity, synchronously.

- 6 Y. P. Zang, F. J. Zhang, C. A. Di and D. B. Zhu, *Mater. Horiz.*, 2015, **2**, 140–156.
- 7 J. W. Zhong, Q. Z. Zhong, Q. Y. Hu, N. Wu, W. B. Li, B. Wang, B. Hu and J. Zhou, *Adv. Funct. Mater.*, 2015, **25**, 1798–1803.
- 8 Q. Z. Zhong, J. W. Zhong, X. F. Cheng, X. Yao, B. Wang, W. B. Li, N. Wu, K. Liu, B. Hu and J. Zhou, *Adv. Mater.*, 2015, **27**, 7130–7136.
- 9 D. D. Han, Y. L. Zhang, H. B. Jiang, H. Xia, J. Feng, Q. D. Chen, H. L. Xu and H. B. Sun, *Adv. Mater.*, 2015, **27**, 332–338.
- 10 W. Wang, Y. Q. Liu, Y. Liu, B. Han, H. Wang, D. D. Han, J. N. Wang, Y. L. Zhang and H. B. Sun, *Adv. Funct. Mater.*, 2017, **27**, 1702946.
- 11 J. J. Yao, *Light: Sci. Appl.*, 2017, **6**, e17062.
- 12 S. Chen, N. Wu, L. Ma, S. Lin, F. Yuan, Z. Xu, W. Li, B. Wang and J. Zhou, *ACS Appl. Mater. Interfaces*, 2018, **10**, 3660–3667.
- 13 K. Liu, Y. S. Zhou, F. Yuan, X. B. Mo, P. H. Yang, Q. Chen, J. Li, T. P. Ding and J. Zhou, *Angew. Chem., Int. Ed.*, 2016, **55**, 15864–15868.
- 14 A. M. Almassri, W. Z. W. Hasan, S. A. Ahmad, A. J. Ishak, A. M. Ghazali, D. N. Talib and C. Wada, *J. Sens.*, 2015, 846487.
- 15 A. V. Tran, X. M. Zhang and B. L. Zhu, *IEEE Trans. Ind. Electron.*, 2018, **65**, 6487–6496.
- 16 H. W. Li, K. J. Wu, Z. Y. Xu, Z. W. Wang, Y. C. Meng and L. Q. Li, *ACS Appl. Mater. Interfaces*, 2018, **10**, 20826–20834.
- 17 Y. Shu, H. Tian, Y. Yang, C. Li, Y. L. Cui, W. T. Mi, Y. X. Li, Z. Wang, N. Q. Deng, B. Peng and T. L. Ren, *Nanoscale*, 2015, **7**, 8636–8644.
- 18 K. Ariga, K. Minami and L. K. Shrestha, *Analyst*, 2016, **141**, 2629–2638.
- 19 D. D. Han, Y. L. Zhang, Y. Liu, Y. Q. Liu, H. B. Jiang, B. Han, X. Y. Fu, H. Ding, H. L. Xu and H. B. Sun, *Adv. Funct. Mater.*, 2015, **25**, 4548–4557.
- 20 G. Ge, Y. C. Cai, Q. C. Dong, Y. Z. Zhang, J. J. Shao, W. Huang and X. C. Dong, *Nanoscale*, 2018, **10**, 10033–10040.
- 21 Y. Liu, L. Q. Tao, D. Y. Wang, T. Y. Zhang, Y. Yang and T. L. Ren, *Appl. Phys. Lett.*, 2017, **110**, 123508.
- 22 S. J. Chen, S. Y. Li, S. Peng, Y. K. Huang, J. Q. Zhao, W. Tang and X. J. Guo, *J. Semicond.*, 2018, **39**, 013001.
- 23 S. M. Doshi and E. T. Thostenson, *ACS Sens.*, 2018, **3**, 1276–1282.
- 24 P. P. Zhang, L. X. Lv, Z. H. Cheng, Y. Liang, Q. H. Zhou, Y. Zhao and L. T. Qu, *Chem. – Asian J.*, 2016, **11**, 1071–1075.
- 25 L. X. Lv, P. P. Zhang, T. Xu and L. T. Qu, *ACS Appl. Mater. Interfaces*, 2017, **9**, 22885–22892.
- 26 L. Sheng, Y. Liang, L. Jiang, Q. Wang, T. Wei, L. Qu and Z. Fan, *Adv. Funct. Mater.*, 2015, **25**, 6545–6551.
- 27 Q. L. Tan, W. Lv, Y. H. Ji, R. J. Song, F. Lu, H. L. Dong, W. D. Zhang and J. J. Xiong, *Sens. Actuators, B*, 2018, **270**, 433–442.
- 28 D. D. Han, Y. L. Zhang, J. N. Ma, Y. Liu, J. W. Mao, C. H. Han, K. Jiang, H. R. Zhao, T. Zhang, H. L. Xu and H. B. Sun, *Adv. Mater. Technol.*, 2017, **2**, 1700045.
- 29 H. T. Cheng, G. Shao, S. Ebadi, X. H. Ren, K. Harris, J. Liu, C. Y. Xu, L. N. An and X. Gong, *Sens. Actuators, A*, 2014, **220**, 22–33.
- 30 J. J. Xiong, Y. Li, Y. P. Hong, B. Z. Zhang, T. H. Cui, Q. L. Tan, S. J. Zheng and T. Liang, *Sens. Actuators, A*, 2013, **197**, 30–37.
- 31 S. Wan, H. C. Bi, Y. L. Zhou, X. Xie, S. Su, K. B. Yin and L. T. Sun, *Carbon*, 2017, **114**, 209–216.
- 32 M. Kang, J. Kim, B. Jang, Y. Chae, J. H. Kim and J. H. Ahn, *ACS Nano*, 2017, **11**, 7950–7957.
- 33 K. Lee, J. Lee, G. Kim, Y. Kim, S. Kang, S. Cho, S. G. Kim, J. K. Kim, W. Lee, D. E. Kim, S. Kang, D. E. Kim, T. Lee and W. Shim, *Small*, 2017, 1700368.
- 34 M. S. Sarwar, Y. Dobashi, C. Preston, J. K. M. Wyss, S. Mirabbasi and J. D. W. Madden, *Sci. Adv.*, 2017, **3**, e1602200.